Research on Liquid Crystal Reflectarray with Reduced Reflection Loss

Hiroyasu SATO[†], Yue CUI[†], Hideo FUJIKAKE[†], and Qiang CHEN[†]

† Graduate School of Engineering, Tohoku University
Aza-Aoba 6–6–05, Aoba-ku, Sendai, 980–8579, Japan.

E-mail: †hiroyasu.sato.b1@tohoku.ac.jp

Abstract In this paper, we investigate the reduction of reflection loss in liquid crystal reflectarray (LCRA). Firstly, a structure that reduces the reflection field by eliminating the electric field in the liquid crystal (LC) is proposed. An air layer is introduced to the reflectarray (RA) structure, and the electric field can be controlled by altering the thickness of the air layer. Measurement results show that the reflection loss is reduced by up to 8.8 dB, while the reflection phase range is also reduced. Then, a bias voltage supply method is proposed to achieve reflection loss reduction without sacrificing the phase range. RResonant structures in the LCRA element is connected to bias lines separately, which achieves independent control of the two resonance. Measurement results indicate that the reflection loss is reduced by up to 17 dB with a 570-degree phase range, validating the proposed method in reducing the reflection loss without phase range degradation.

Key words Liquid crystal, phase range, reflectarray, reflection loss.

1. Introduction

Reflectarray (RA) is an effective means to increase the level of electromagnetic signal (EM) in the target area without excessive power consumption, and its two-dimensional arrangement makes it easy to integrate into structures such as facades of buildings and interior walls [1, 2]. To meet the complex coverage requirements, the RA which can change beam direction has gained widespread attention. Numerous studies on RA have been conducted so far [3–6], including such as the use of diodes, mechanical methods and nematic liquid crystal (LC). The rod-shaped molecular structure of nematic LC can be deflected continuously by an external electric or magnetic field, resulting in a corresponding continuous change in its permittivity. This feature of LC allows RA to continuously shift the beam direction, which is the primary advantage of liquid crystal reflectarray (LCRA).In addition, the ease of applying an external electric field to the LC through bias lines further contributes to the design simplicity and cost-effectiveness of the LCRA.

To improve response speed and achieve low-voltage operation, it is necessary to make the liquid crystal layer thinner. However, making the liquid crystal layer thinner increases the high-frequency electric field inside the liquid crystal, which increases reflection loss. Reflection loss not only results in dissipation of the incident EM wave but also introduces significant variations in reflection magnitude at different reflection phases, leading to a decrease in the aperture efficiency of LCRA [7].

As one of effective method for minimizing the increase in reflection loss even when making the liquid crystal layer thinner is to reduce the Q value of the patch elements of the reflectarray [8], [9], but there is a limit to reduce loss by selecting the structure of patch elements. To address this issue, a novel structure by introducing an air layer beneath the LC layer is proposed. Simulated and measured results show that the thickness of the air layer affects the reflection loss and magnitude variation of the LCRA. Additionally, 3D printed fixture is used to control the thickness of the air layer in a cost-effective manner. The proposed LCRA structure has reduced reflection loss, low cost, and easy processing characteristics. On the other hand, the proposed structure suffers from a disadvantage that the reflection phase range decreases as the loss reduced.

To reduce the reflection loss without decreasing the phase range, a novel RIS-LC unit cell using a dual-bias voltage supply method is proposed. Two bias lines are introduced to control the LC permittivities beneath two resonant structures with different sizes, thereby enabling independent control of each structure's resonance. Through this approach, one reflection phase can correspond to multiple reflection magnitudes, allowing for the selection of optimal magnitudes across all phases. Consequently, the proposed RIS-LC can achieve a reduction of reflection loss without compromising the phase range, while maintaining a simple structure.

2. Low Loss Design by Introducing Air Layer

2.1 Proposed structure

The proposed LCRA unit cell structure is shown in Fig. 1. It consists of four parts arranged from top to bottom as shown in Fig. 1(a): the superstrate, the LC layer, the substrate, the air layer, and the metal ground. Two identical metal patches are positioned on the upper and lower surfaces of the LC layer, with each patch connected to a bias line to apply bias voltage, as shown in Fig.1 (b) and (c). The relative permittivity ($\varepsilon_{r\perp}$) of the LC without bias voltage is 2.5, and the loss tangent ($\tan \delta_{\perp}$) is 0.02. Conversely, when the full bias voltage is applied, the relative permittivity ($\varepsilon_{r//}$) and loss tangent ($\tan \delta_{//}$) are 3 and 0.007, respectively. Additionally, to ensure smooth surfaces for the polymide film coating process, glass ($\varepsilon_r = 3.7$, $\tan \delta = 0.007$) is chosen as the material for both the superstrate and substrate.

2.2 Theoretical Analysis

When electromagnetic waves traverse a dielectric medium, a portion of their energy dissipates due to the inherent conductivity (σ) of the dielectric material [10].

$$P_{loss} = \frac{\sigma}{2} \iiint_v |\boldsymbol{E}|^2 dv \tag{1}$$
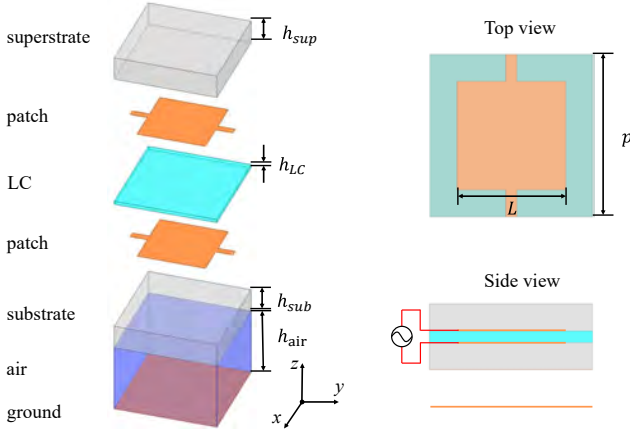
Fig. 1 The proposed LCRA unit cell structure.

where P_{loss} represents the time-average dissipated power. In the case of LCRA, the dissipation of incident energy in LC, as well as other substrates and metals, is referred to as reflection loss. Due to the high loss tangent ($\tan\delta = \sigma/\omega\varepsilon$) exhibited by LC, the LCRA reflection loss is primarily attributed to the energy dissipated in LC. To address this challenge, the proposed LCRA unit cell integrates an air layer beneath the LC layer. It enables a reduction in the electric field while maintaining a thin LC layer, without incurring additional costs.
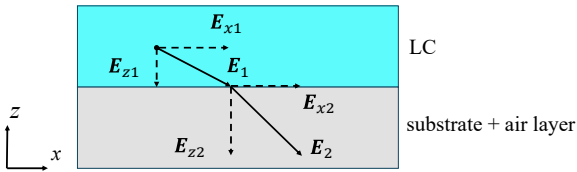
Fig. 2 The schematic of electric field at the interface between the LC layer and the substrate.

When a plane EM wave illuminates the proposed LCRA, the metal patch generates induced current. Subsequently, the induced current excites an electric field [11]. The schematic of electric field at the interface between the LC layer and the substrate is shown in Fig.2. For simplicity, E_y is adopted to represent the parallel component. According to the Maxwell-Faraday equation and the Gauss's law [12], the parallel and perpendicular components at the interface can be written as:

$$|E_{x1}| = |E_{x2}| \tag{2}$$

$$\frac{\varepsilon_1}{\varepsilon_{LC}} = \frac{|E_{z1}|}{|E_{z2}|} \tag{3}$$

where ε_{LC} and ε_1 represent the permittivity of the LC and the effective permittivity of the substrate and the air layer. The electric field in the LC layer decreases as ε_1 reduces. This reduction in ε_1 can be achieved by adjusting the thickness of the air layer (h_{air}) [13]:

$$\varepsilon_1 = \frac{(h_{sub} + h_{air})\varepsilon_{sub}\varepsilon_{air}}{h_{sub}\varepsilon_{air} + h_{air}\varepsilon_{sub}} \tag{4}$$

where ε_{sub} and ε_{air} represent the permittivity of the substrate and the

air layer, respectively. Increasing the thickness of the air layer (h_{air}) causes the ε_1 to decrease and converge to ε_0. Consequently, the electric field in the LC layer and the reflection loss of the proposed LCRA decrease with increasing h_{air}.
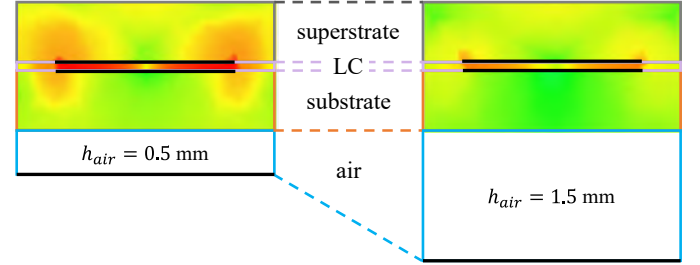
Fig. 3 The simulated electric field of the proposed LCRA unit cell.

The aforementioned theoretical analysis was validated through full-wave simulation.Fig. 3 illustrates the simulated electric field for the various thicknesses of air layer. The electric field within LC layer decreases as the h_{air} increases from 0.5mm to 1.5mm, which is consistent with the theoretical analysis. The reduction in electric field within the LC layer leads to reduced reflection loss.

2.3 Measurement

A 15×15 prototype LCRA was fabricated, comprising three main components: the superstructure, the metal ground, and 3D printed fixtures, as depicted in Fig. 4 (a). The superstructure is composed of the superstrate, the LC layer, and the substrate. Fig. 4 (b) shows the side view of the assembled LCRA. The air layer is formed by the 3D printed fixtures, and the thickness can be adjusted by using different fixtures. The reflection loss and phase range of the prototype LCRA were measured using a lens-loaded printed antipodal fermi tapered slot antenna (APFA) [14] with Keysight boldsymboltor Network Analyzer P5008A. The permittivity of the LC was adjusted by applying a low-frequency voltage of 1 kHz to the electrodes (i.e., patches).

Fig. 5 presents the measurement results for various air layer thicknesses. As shown in Fig. 5 (a), increasing the h_{air} leads to a reduction in reflection loss. Compared to $h_{air} = 0.5$ mm, there is an 8.8 dB reduction in reflection loss when no bias voltage is applied ($\varepsilon_{r\perp}$), and a 3 dB reduction at full bias voltage ($\varepsilon_{r//}$). Fig. 5 (b) shows that the reflection phase range decreases from 290 degrees to 204 degrees as the h_{air} increases from 0.5 mm to 1.5 mm.

The reflection magnitude and phase versus bias voltage were also measured to evaluate the proposed LCRA structure, as shown in Fig. 5 (c) and (d). The frequency was fixed at 40.3 GHz, and the air layer thicknesses were chosen as 0.5 mm, 1 mm, and 1.5 mm, respectively. The reflection magnitude variation reduced from 11.9 dB at $h_{air} = 0.5$ mm to 3.4 dB at $h_{air} = 1.5$ mm. Meanwhile, the phase variation reduced from 275 degrees at $h_{air} = 0.5$ mm to 204 degrees at $h_{air} = 1.5$ mm. The measured results validating the effectiveness of the proposed structure for reducing the reflection loss of LCRA and there has a trade-off between the reflection loss and the phase range.

3. Low Loss Design with Dual-bias Voltage

3.1 Proposed structure

To address the issue of the trade-off relationship between the reflection loss and the phase range, another RA element is proposed. The LCRA unit structures of the proposed and single bias supply methods are illustrated in Fig. 6, comprising a superstrate layer, an LC layer, and a metal ground. The single bias voltage supply method

(a)

(b)

(c)
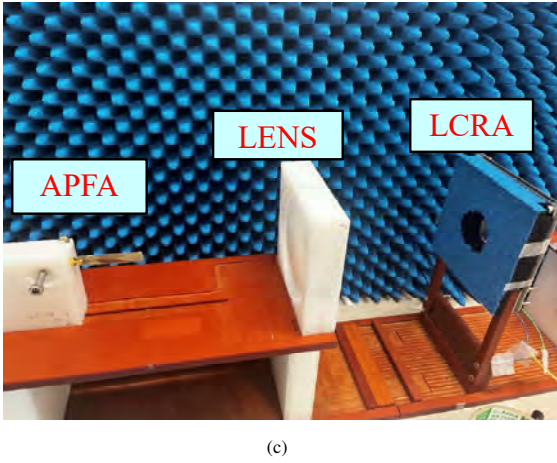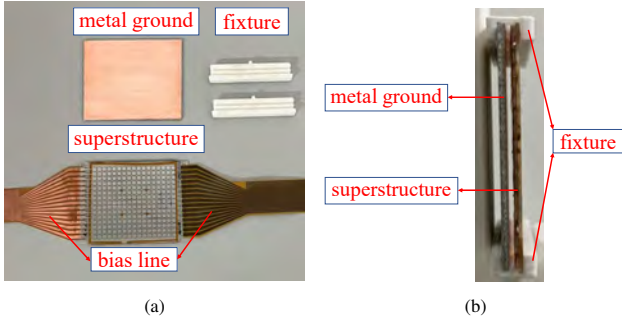
Fig. 4　(a) Unassembled and (b) side view of the assembled proto-type LCRA.

(a)　　　　　　　　(b)

(c)　　　　　　　　(d)
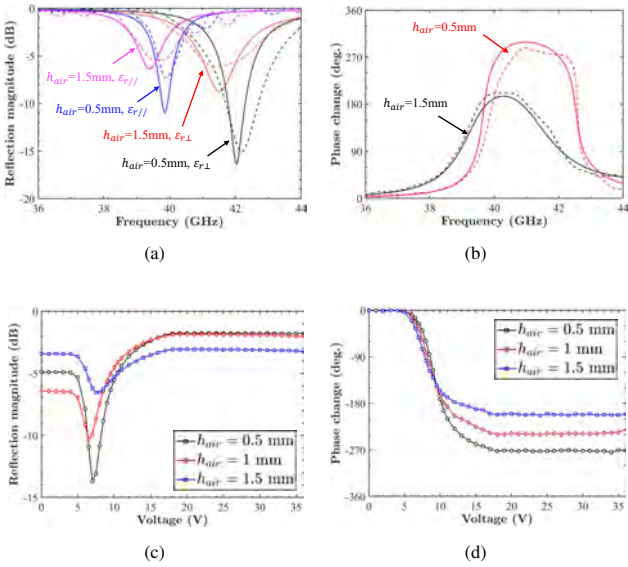
Fig. 5　Measured (a) reflection magnitude and (b) reflection phase range versus frequency, (c) reflection magnitude and (d) reflection phase versus bias voltage at 40.3 GHz.

uses single bias line to control two resonant structures, while the proposed method control the two resonant structures independently by two bias lines, as shown in Fig. 6(a). This arrangement enables independent control of the resonance states of the two resonant structures via two different bias voltages (V_1 and V_2).The LC and the material for the superstrate is same as the previously proposed element.

(a)

(b)
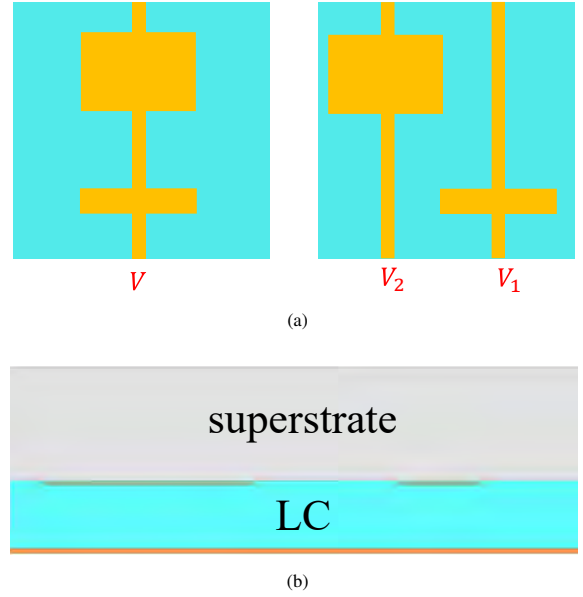
Fig. 6　Top view of the (a) single bias voltage supply method and the proposed method. (c) Side view of the LCRA unit cell.

3.2　Results and discussions

A 12×13 LCRA prototype controlled by the proposed bias voltage supply method is fabricated. the prototype is shown in Fig. 7(a), and the responses of LC under different bias voltages V_1 and V_2 are shown in Fig. 7(b). It can be seen that the edge of the two resonant structures are brightened individually, which means the two resonant structure are controlled independently. Fig. 8 illustrates the measured performances of single and dual bias voltage supply methods at 41 GHz. The reflection magnitude and phase under different LC relative permittivity of the single bias method are shown in Fig 8(a) and (b). As can be seen, the single bias method exhibits a phase variation of 570° , but with high reflection loss (up to 24.7 dB) where the phase ranges rapidly. Fig. 8(c) display the comparison of the reflection coefficient of the two method in smith chart at 41 GHz. It is evident that in the proposed method, the reflection phase and magnitude exhibit a one-to-multiple correspondence for the LC permittivity. The reflection phase range is the same as the single bias method, and the independent control allows one phase mapped to multiple value sets of $(\varepsilon_{r1}, \varepsilon_{r2})$. Consequently, the optimal reflection magnitude can be chosen from these value sets to obtain low reflection loss.

For demonstration, the optimum reflection magnitude to all phase under single and dual bias voltage supply methods at 41 GHz are depicted in Fig. 9(a). It can be seen that across the all 360° phase, the reflection magnitude under the proposed method obtains a higher reflection magnitude than single bias method, with a maximum improvement of 17 dB. Calculated bistatic radar cross section (bRCS) of the two method under 0° incident are shown in Fig. 9(b). It can be seen that up to 30° beam steering, the proposed method has a larger bRCS by up to 7.94 dB than single bias method, validating that the proposed method reduces the reflection loss and allows LCRA reflect more energy to the target direction.

4.　Conclusion

Two element structure is proposed to reduce the reflection loss in LCRA. The first structure introducing an air layer beneath the LC layer. Theoretical analysis demonstrates a direct correlation between the effective permittivity of the air layer and the electric field
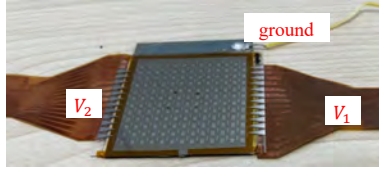
(a)
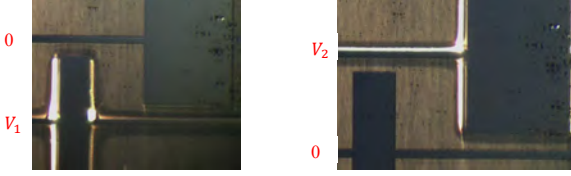
(b)

Fig. 7　(a) The prototype of the proposed LCRA and (b) the responses of LC under different bias voltages.
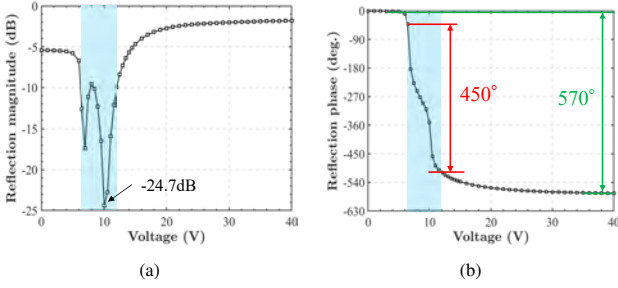
(a)

(b)
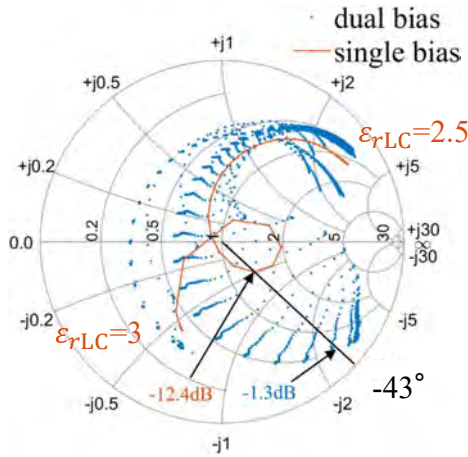
(c)

Fig. 8　(a) The reflection and (b) phase of the single bias voltage method. (c) The comparison of the two method in smith chart at 41 GHz.

within the LC layer, subsequently influencing the reflection loss of the LCRA. Modulating the air layer's thickness within the air layer allows precise control over the effective permittivity, thus offering a means to diminish the LCRA's reflection loss. A 15×15 prototype array of the proposed LCRA structure is fabricated, experiment results indicated that the structure effectively reduces the reflection loss and magnitude variation of the LCRA, while the phase range decreases as the reflection loss is reduced. To achieve independent control of the reflection magnitude and phase, the second proposed element structure is proposed. The two resonant structure is connected to one bias line respectively, realizing dual-bias voltage supply. As a result, the reflection magnitude and phase could be controlled in-
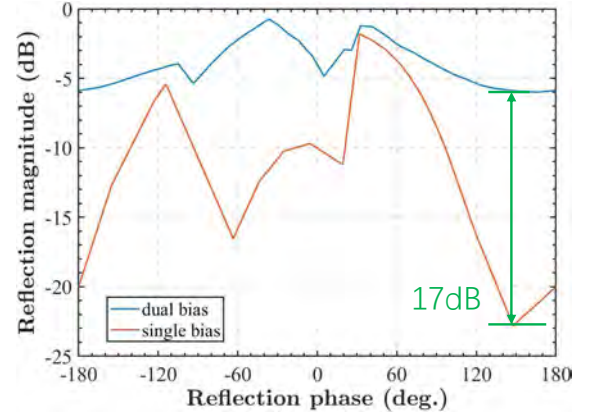
(a)
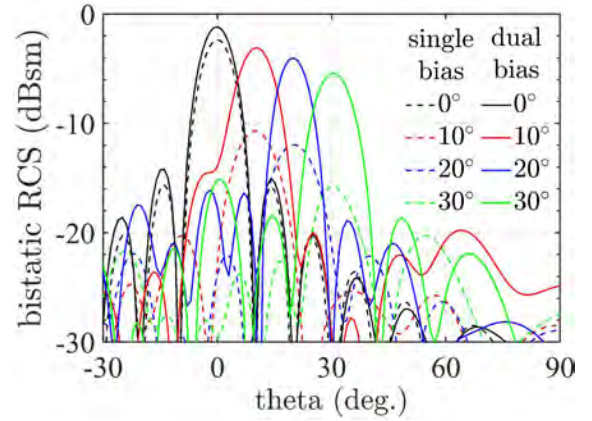
(b)

Fig. 9　(a) The reflection and (b) phase of the single bias voltage method. (c) The comparison of the two method in smith chart at 41 GHz.

dependently by the proposed method. By selecting the optimum values of reflection magnitude on each phase, significant reflection loss reduction is achieved by up to 17 dB without phase range decreasing. The proposed LCRA structure has advantages of low-loss, large phase range, cost-effective and easy processing, which making it a promising candidate for practical applications.

5.　Acknowledgment

References

[1]　D. Berry, R. Malech, and W. Kennedy, "The reflectarray antenna," *IEEE Trans. Antennas Propag.*, vol. 11, no. 6, pp. 645–651, 1963.

[2]　D. Pozar, S. Targonski, and H. Syrigos, "Design of millimeter wave microstrip reflectarrays," *IEEE Trans. Antennas Propag.*, vol. 45, no. 2, pp. 287–296, 1997.

[3]　W. Wu, K.-D. Xu, Q. Chen, T. Tanaka, M. Kozai, and H. Minami, "A wideband reflectarray based on single-layer magneto-electric dipole elements with 1-bit switching mode," *IEEE Trans. Antennas Propag.*, vol. 70, no. 12, pp. 12 346–12 351, 2022.

[4]　J. Han, L. Li, G. Liu, Z. Wu, and Y. Shi, "A wideband 1 bit 12 × 12 reconfigurable beam-scanning reflectarray: Design, fabrication, and measurement," *IEEE Antennas Wireless Propag. Lett.*, vol. 18, no. 6, pp. 1268–1272, 2019.

[5]　W. Menzel, D. Pilz, and M. Al-Tikriti, "Millimeter-wave folded re-

flector antennas with high gain, low loss, and low profile," *IEEE Antennas Propag. Mag.*, vol. 44, no. 3, pp. 24–29, 2002.

[6]   S. Bildik, S. Dieter, C. Fritzsch, W. Menzel, and R. Jakoby, "Reconfigurable folded reflectarray antenna based upon liquid crystal technology," *IEEE Trans. Antennas Propag.*, vol. 63, no. 1, pp. 122–132, 2015.

[7]   P. Nayeri, F. Yang, and A. Z. Elsherbeni, *Reflectarray antennas: theory, designs, and applications.*   John Wiley & Sons, 2018.

[8]   H. Sato, R. Matsuda, H. Fujikake, and Q. Chen, "Low-sidelobe design of intelligent reflecting surface using liquid chrystal," *Proc. 2024 International Symposium on Antennas and Propagation (ISAP 2024)*.

[9]   H. Sato, T. Fujisawa, Y. Shibata, T. Ishinabe, H. Fujikake, and Q. Chen, "Design of intelligent reflect surface using liquid crystals," *Proc. 35th URSI General Assembly and Scientific Symposium (URSI GASS 2023)*.

[10]   W. L. Stutzman and G. A. Thiele, *Antenna theory and design.*   John Wiley & Sons, 2012.

[11]   C. A. Balanis, *Antenna theory: analysis and design.*   John wiley & sons, 2016.

[12]   D. Pozar, *Microwave Engineering, 4th Edition.*   Wiley, 2011.

[13]   M. F. Iskander, *Electromagnetic fields and waves.*   Prentice Hall, 1992.

[14]   H. Sato, Y. Takagi, and K. Sawaya, "High gain antipodal fermi antenna with low cross polarization," *IEICE transactions on communications*, vol. 94, no. 8, pp. 2292–2297, 2011.